CORROSION SCIENCE AND TECHNOLOGY, Vol.9, No.5(2010), pp.196~200

Oxidation Behaviors of Porous Ferritic Stainless Steel Support for Metal-supported SOFC

I. J. Moon†, J. W. Lee, H. J. Cho[1], G. M. Choi[1], and H. K. Sohn

Pohang Institute of Metal Industry Advancement, 166-5, Jigokdong, Gyeongbuk, 790-390, Korea
[1]Pohang University of Science and Technology, San 31, Hyojadong, Gyeongbuk, 790-784, Korea
(Received March 25, 2010; Revised September 28, 2010; Accepted September 30, 2010)

Recently porous metal has been used as supporting metal in planar type SOFC. In order to search optimum alloys for porous metal support and estimate the stability of metal-supported SOFC at high temperature, it is necessary to investigate the oxidation behaviors of porous material for metal support in comparison with dense material. Oxidation tests of porous and dense stainless steels were conducted at 600 ℃ and 800 ℃. Since the specific surface area of porous material is much larger than that of dense material, surface area should be considered in order to compare the oxidation rate of porous stainless steel with that of dense stainless steel. The specific surface area of porous body was measured using image analyzer. The weight gain of porous stainless steel was much greater than those of dense stainless steels due to its larger specific surface area. Considering the specific surface area, the oxidation rate of porous stainless steel is likely to be the same as that of dense stainless steel with the same surface area. The change in chromium content in stainless steel during oxidation was also investigated. The experimental result in chromium content in stainless steel during oxidation corresponded with the calculated value. While the change in chromium content in dense stainless steel during oxidation is negligible, chromium content in porous stainless steel rapidly decreases with oxidation time due to its large specific surface area. The significant decrease in chromium content in porous stainless steel during oxidation may affect the oxidation resistance of porous stainless steel support and long term stability of metal-supported SOFC.

Keywords *: Ferritic stainless steel, metal support, SOFC, oxidation, porous metal*

1. Introduction

Solid oxide fuel cell (SOFC) is very promising energy conversion device due to its high electrical efficiency and fuel flexibility. Recently, advanced technologies of electrolyte and electrode allow lower operating temperature of SOFC, making it possible to use metal support for SOFC. Metal-supported SOFC is expected to be competitive in fuel cell market because of the strength, tolerance to rapid thermal cycling, and reduced cost.[1)~4)]

FeCr-based ferritic stainless steels are the preferred metallic support material due to their low cost, adequate coefficient of thermal expansion (CTE) match with electrolyte such as YSZ.[1)] Recently porous steel has been used as supporting metal in planar type SOFC.[5)~7)] Villarreal et al.[5)] built cells on porous Fe-30 wt%Cr steel substrate, that was pre-fired at 400 ℃ and then Ni-YSZ anode layer was tape-casted, pre-fired at 600 ℃ and sprayed with an electrolyte. After that, the cells were co-sintered at 1350 ℃ in H_2.

It is reported that while dense material can operate under the working conditions of the SOFC, porous material still needs a new alloy design due to its large specific surface area.[2),8)] In order to search optimum alloys for the porous metal support and estimate the stability of metal-supported SOFC at high temperature, it is necessary to investigate the oxidation behavior of porous material for metal support in comparison with dense material.

Optical microscopy and image analyzer were used to measure the specific surface area of porous body. Considering the specific surface area, the oxidation rate of porous stainless steel was compared with those of other dense stainless steels. Chromium depletion in the stainless steel by outward diffusion of chromium for the formation of chromium oxide during oxidation was also investigated to confirm the validity of STS430 powder as a material for support in metal-supported SOFC.

† Corresponding author: iljoon@postech.ac.kr

Table 1. Chemical composition of ferritic stainless steel (STS430) in wt%

material	C	Si	Mn	P	Cr	Ni	Mo	Cu	Al
powder	0.011	1.04	0.064	0.0077	16.80	0.25	0.014	0.016	0.0039
dense	0.034	0.26	0.516	0.0290	15.94	0.134	0.034	0.028	0.0020

Table 2. Particle size and apparent density of stainless steel powder

Material	Mesh	Avg. particle size (㎛)	Apparent density (g/cc)
STS430	-270 ~ +325	45	2.69

2. Experimental methods

2.1 Material

STS 430 was used as a material for the experiment due to its low cost, adequate coefficient of thermal expansion (CTE) match with electrolyte such as YSZ. STS 430 powder was made by water atomization method. Powders with the particle size being larger than 270 mesh are difficult to fabricate tape by tape casting process, and powders with the particle size being smaller than 400 mesh are almost completely sintered during sintering process due to their fine particle size. So, powders with the particle size ranging from 275 to 325 mesh were used to fabricate thin porous stainless steel tape of 18 mm diameter and 100 μm thickness.

In order to compare the oxidation behavior of porous stainless steel with that of dense stainless steel, dense STS430 of 20 x 20 x 2 mm^3 was also used for oxidation test. Chemical compositions of the ferritic stainless steels and physical properties of the powder are shown in Table 1 and 2, respectively.

2.2 Tape casting and sintering

Thin green layer for support was fabricated by using tape casting method. Binder solution used for the tape casting was composed of toluene, ethanol, polyvinyl butyral (PVB, B-74), and dioctyl phthalate. Slurry was prepared by ball milling a mixture of powders and binder solution for 24 hr. Then the tape was de-bound at 400 ℃ for 1 hr and sintered at 1300 ℃ for 3 hr in reducing atmosphere (5%H_2-Ar).

2.3 Oxidation test and analysis

The sintered stainless steel tapes and the dense stainless steels were oxidized at 600 ℃ and 800 ℃ in air. Oxide phases formed by oxidation were characterized by X-ray diffraction (XRD). Cross section of the oxidized stainless steel was examined by field emission-scanning electron microscopy (FE-SEM) with energy dispersive X-ray analysis (EDX) to see the oxide layer and chromium concentration profile in the stainless steel. Optical microscopy and image analyzer were used to measure the specific surface area of the porous stainless steel tape after oxidation.

3. Results and discussion

SOFC is generally operated at the temperature range of 600~800 ℃. It is reported that operating at 600 ℃ imposes far less severe corrosion constraints on the ferritic stainless steel than sustained operation at 800 ℃.[9] Increasing operating temperature enhances the cell performance. The increased temperature in turn increases the rate of chromia scale growth in the metal, leading to break-away oxidation and destruction of the cell.[2] Oxidation tests of porous and dense stainless steels were conducted at 600 ℃ and 800 ℃ in this work.

XRD and cross-sectional images of the porous stainless steel tapes oxidized at 600 ℃ and 800 ℃ for 24 hr are shown in Figure 1 and 2. Cr_2O_3 oxide layer was observed in the sample oxidized at 800 ℃ for 24 hr. In case of the oxidation at 600 ℃ for 24 hr, no oxide was detected. In order to investigate further oxidation behaviors of porous stainless steel for metal support in comparison with dense stainless steel, oxidation tests were conducted at 800 ℃ for 500 hr.

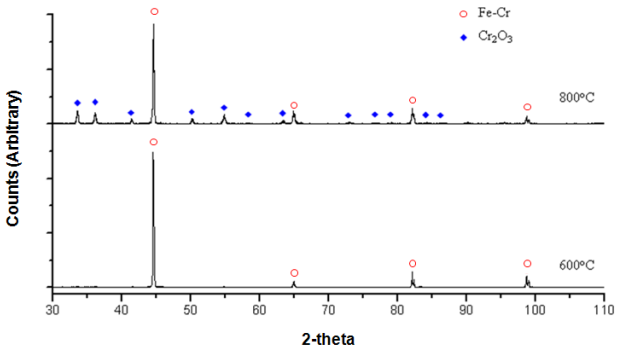

Fig. 1. X-ray diffraction patterns of porous STS 430 tape oxidized for 24hr in air.

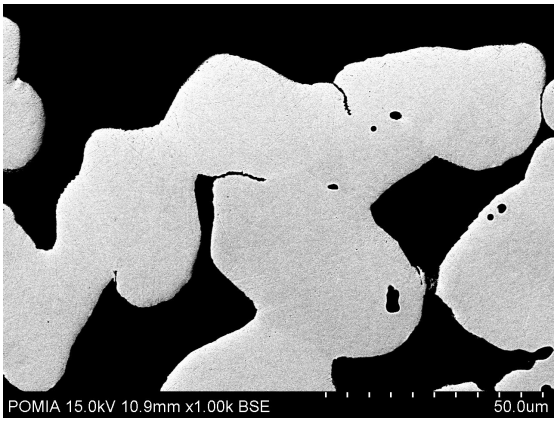

(a) 600℃

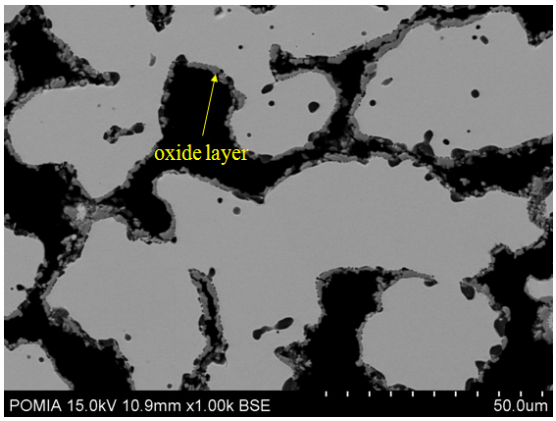

(b) 800℃

Fig. 2. Cross-sectional images of porous STS 430 tape oxidized for 24 hr in air.

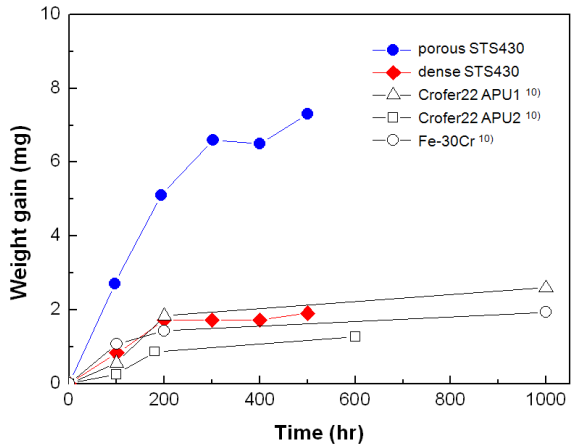

Fig. 3. Weight gain of ferritic stainless steels oxidized at 800℃ in air.

The weight gain of the porous stainless steel at 800 ℃ in air is shown in Fig. 3 with those of other dense ferritic stainless steels. In the case of the dense stainless steel, the weight gain was obtained from the present experiment and previous works.[10] The weight gain of the porous stainless steel was much greater than those of dense ferritic stainless steels due to its larger specific surface area. It is doubtful whether the oxidation rate of porous stainless steel is still higher than that of dense stainless steel with the same surface area.

In order to compare the oxidation rate of porous stainless steel with that of dense stainless steel, the specific surface area of the porous body should be measured. In this work, BET could not be used to measure the specific surface area of the porous stainless steel tape because its pore volume was too small. Optical microscopy and image analyzer were used to measure the specific surface area of the porous stainless steel. The specific surface area of the porous stainless steel is as followings.

$$\text{Specific surface area} = \frac{S}{m} = \frac{1}{\rho}\left(\frac{S}{V}\right) \ [\text{cm}^2/\text{g}] \qquad (1)$$

where, S is surface area of the particle,
m is mass of the particle,
ρ is density of the stainless steel.

The specific surface area of the porous stainless steel can be related to the 2-dimensional cross-sectional image as followings, assuming that the particles are spherical.

$$\text{Specific surface area} = \frac{3}{2\rho}\left(\frac{l}{a}\right) \ [\text{cm}^2/\text{g}] \qquad (2)$$

where, l and a are perimeter and cross-sectional area of the particle, which were measure by image analyzer.

The specific surface area of the porous stainless steel tape calculated by equation (2) is listed in Table 3. The specific surface area at each oxidation time was used to evaluate the oxidation rate of the porous stainless steel. The oxidation rate of the porous stainless steel is shown in Fig. 4 with those of other dense ferritic stainless steels. Considering the specific surface area, the oxidation rate of the porous stainless steel was in the similar range with

Table 3. Specific surface area of porous STS 430 tape oxidized at 800 ℃ in air

Oxidation time (hr)	Specific surface area (cm^2/g)
100	141
200	138
300	98
400	88
500	90

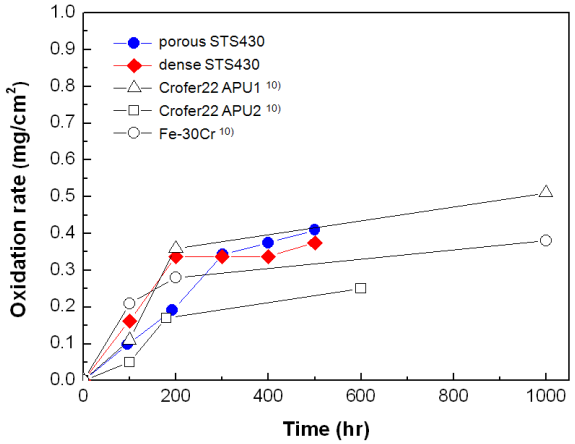

Fig. 4. Oxidation rates of ferritic stainless steels oxidized at 800℃ in air.

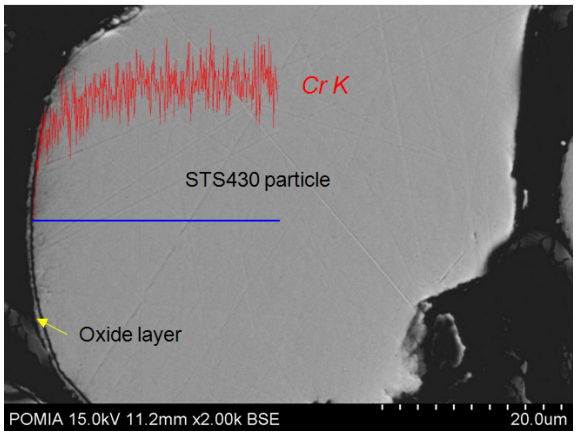

Fig. 5. Chromium concentration profiles in STS 430 powder after 3 hr at 800℃ in air.

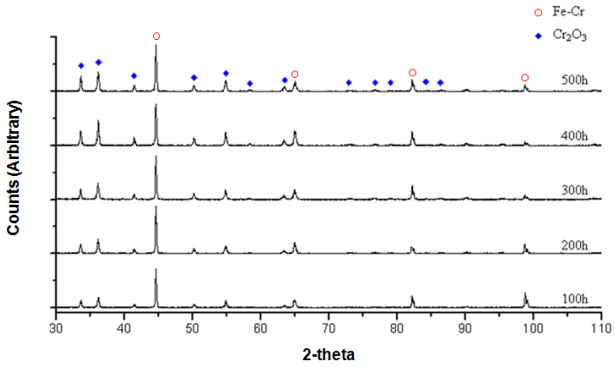

Fig. 6. X-ray diffraction patterns of porous STS 430 tape oxidized at 800℃ in air.

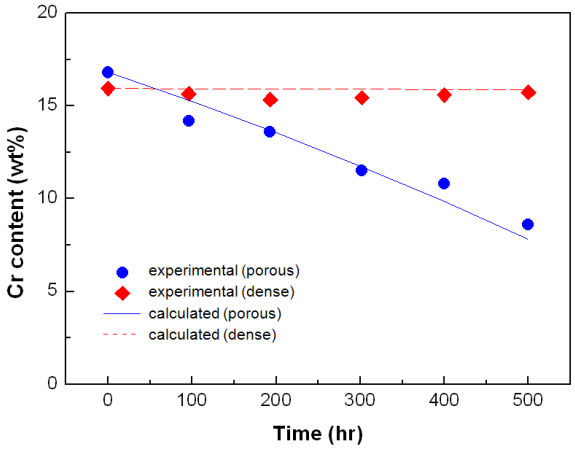

Fig. 7. Chromium content in STS430 during oxidation at 800℃ in air.

those of other dense ferritic stainless steels. The oxidation rate of porous stainless steel is likely to be the same as that of dense stainless steel with the same surface area. However, the decrease in chromium content in stainless steel during oxidation may be significant in the porous stainless steel due to its large specific surface area.

The change in chromium content in the stainless steel during oxidation was investigated to confirm the validity of ferritic stainless powder as a material for support in metal-supported SOFC. EDX line scan was conducted to see chromium concentration profile in the stainless steel powder during oxidation. The EDX line scans are shown in Fig. 5. After 3 hr oxidation at 800 ℃ in air, chromium depletion in the stainless steel near the interface of oxide and metal is observed, which is due to the outward diffusion of chromium for the formation of chromium oxide. Chromium content in the stainless steel is expected to decrease as oxidation proceeds due to the outward diffusion of chromium.

Fig. 6 shows XRD of the porous stainless steel tape oxidized at 800 ℃ in air. Up to 500 hr oxidation, no other oxide was detected except Cr_2O_3 oxide. Chromium content in the stainless steel during oxidation was calculated, assuming that the growth rate of Cr_2O_3 oxide is 1.5 μm/500 hr which was determined from cross-sectional image of FE-SEM after oxidation. The chromium content was analyzed by EDX at the center (~20 μm apart from surface) of the cross-sectioned particle in the porous stainless steel, and at the center of the cross-sectioned sample in the dense stainless steel. Fig. 7 shows the calculated and experimental chromium content in the stainless steel during oxidation at 800 ℃ in air. The experimental result for chromium content in the stainless steel corresponded with the calculated value.

In the case of dense stainless steel, the change in chromium content in the stainless steel was less than 0.1 wt% after 500 hr oxidation. But, the chromium content in the porous stainless steel rapidly decreased with oxidation

time due to its large specific surface area. After 500 hr oxidation, the chromium content in the porous stainless steel was 7.8 wt%, showing 9 wt% difference in comparison with the initial chromium content in the porous stainless steel. The significant decrease in chromium content in the porous stainless steel during oxidation may affect the oxidation resistance of porous stainless steel support and long term stability of metal-supported SOFC.

4. Conclusions

1) The weight gain of porous stainless steel is much greater than that of dense stainless steel due to its larger specific surface area. Considering the specific surface area, the oxidation rate of porous stainless steel is likely to be the same as that of dense stainless steel with the same surface area.

2) The significant decrease in chromium content in porous stainless steel during oxidation may affect the oxidation resistance of porous stainless steel support and long term stability of metal-supported SOFC.

Acknowledgements

This work was supported by New & Renewable Energy R&D program (2008-N-FC08-J-01-0-000) under the Ministry of Knowledge Economy, Republic of Korea.

References

1. M.C. Tucker, G.Y. Lau, C. P. Jacobson, L.C. DeJonghe, and S.J. Visco, *J. Power Sources*, **171**, 477 (2007).
2. M.C. Tucker, T.Z. Sholklapper, G.Y. Lau, L.C. DeJonghe, and S.J. Visco, *ECS Trans.*, **25**, 673 (2009).
3. H.Y. Cho, Y.M. Park, and G.M. Choi, *ECS Trans.*, **25**, 695 (2009).
4. P. Blennow, J. Hjelm, T. Klemenso, A. Persson, K. Brodersen, A.K. Srivastava, H.L. Frandsen, M. Lundberg, S. Ramousse, and M. Mogensen, *ECS Trans.*, **25**, 701 (2009).
5. I. Villarreal, C. Jacobson, A. Leming, Y. Matus, S. Visco, and L. De Jonghe, *Electrochem. Solid-State Lett.*, **6**, A78 (2003).
6. Y.B. Matus, L. De Jonghe, C.P. Jacobson, and S.J. Visco, *Solid State Ionics*, **76**, 443 (2005).
7. J.D. Carter, J.M. Bae, T.A. Cruse, J.M. Ralph, and D.J. Myers, US Patent Application, 0251947 A1 (2006).
8. S. Molin, B. Kusz, M. Gazda, and P. Jasinski, *J. Power Sources*, **181**, 31 (2008).
9. N.P. Brandon, D. Corcoran, D. Cummins, A. Duckett, K. El-Khoury, D. Haigh, R. Leah, G. Lewis, N. Maynard, T. McColm, R. Trezona, A. Selcuk, and M. Schmidt, *Journal of Materials Engineering and Performance*, **13**, 253 (2004).
10. I. Antepara, I. Villarreal, L.M. Rodrigeuz-Martinez, N. Lecanda, U. Castro, and A. Laresgoiti, *J. Power Sources*, **151**, 103 (2005).